Emerging Postsynthetic Improvements of BiVO$_4$ Photoanodes for Solar Water Splitting

Lamm, Benjamin; Trześniewski, Bartek J.; Döscher, Henning; Smith, Wilson A.; Stefik, Morgan

Important note
To cite this publication, please use the final published version (if applicable).
Please check the document version above.

PERSPECTIVE

Emerging Postsynthetic Improvements of BiVO₄ Photoanodes for Solar Water Splitting

Benjamin Lamm,[⊥,†] Bartek J. Trześniewski,[⊥,‡] Henning Döscher,[§] Wilson A. Smith,[*,‡] and Morgan Stefik[*,†]

[†]Chemistry and Biochemistry, University of South Carolina, 541 Main Street, Columbia, South Carolina 29208, United States

[‡]Materials for Energy Conversion and Storage (MECS), Department of Chemical Engineering, Delft University of Technology, Van der Maasweg 9, 2629 HZ Delft The Netherlands

[§]Fraunhofer Institute for Systems and Innovation Research ISI, Breslauer Strasse 48, Karlsruhe, Baden-Württemberg 76139, Germany

ABSTRACT: Solar-assisted water splitting with bismuth vanadate (BiVO₄) photoanodes has progressed significantly with many efforts devoted to improving charge separation and surface charge injection through synthetic methods, including dopants and catalytic layers. In contrast, postsynthetic treatments occur after the synthesis of electrodes. Recently, such postsynthetic treatments based upon illumination, chemistry, electrochemistry, or combinations thereof have led to dramatic improvements in the performance and efficiency of BiVO₄ photoanodes. This Perspective summarizes recent BiVO₄ postsynthetic treatments with mechanistic details and highlights important future directions. One broad challenge is that multiple interpretations of defect changes may be consistent with routine X-ray photoelectron spectroscopy data. Further experiments are suggested to better differentiate between the proposed defect changes. Also, performance changes are considered separately with respect to charge separation and charge injection efficiencies as well as within the context of known synthetic modifications. The emergence of postsynthetic treatments highlights new opportunities to understand and improve photoelectrodes. Similar mechanisms may be of further utility as researchers turn more focus toward the development of novel multinary metal oxide photoabsorbers for the production of solar fuels. Lastly, postsynthetic treatments also elucidate possible electrode changes under extended service and can provide new strategies to enable extended device performance.
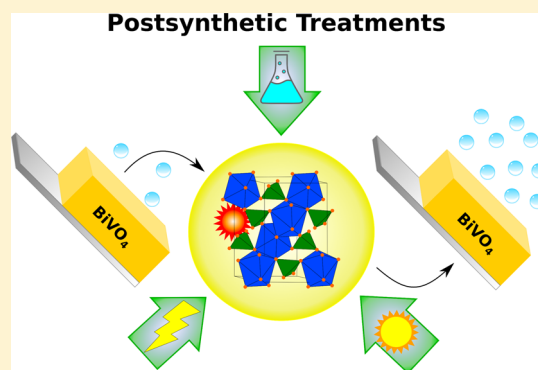
Monoclinic bismuth vanadate (BiVO₄) is a promising and widely studied photoanode for solar-assisted water splitting[1,2] and is made from cheap source compounds. BiVO₄ has an indirect band gap energy of approximately 2.4−2.5 eV (∼500−520 nm band edge),[3,4] with absorption into the visible and ultraviolet (UV) range of light, and with a maximum theoretical photocurrent of ∼7 mA cm⁻² under 1 sun AM 1.5G illumination. Additionally, a wider direct band gap (ca. 2.7 eV) is also present in BiVO₄.[4] The conduction band edge (CB) lies near 0 V_RHE (versus reversible hydrogen electrode), placing the valence band edge (VB) near 2.4 V_RHE and providing significant excess potential for holes to photo-oxidize water while electrons maintain a potential appropriate for hydrogen evolution at the counter electrode with moderate external bias. A thorough review of BiVO₄ photoelectrochemical (PEC) properties and challenges was recently published.[3] Postsynthetic treatments have recently emerged as a way to significantly improve PEC performance with treatments that occur after the synthesis of electrodes. These postsynthetic treatments are based upon illumination, chemistry, electrochemistry, or combinations thereof, improving the PEC performance of active materials in ways that typically cannot be achieved via direct fabrication methods. This Perspective highlights recent findings with BiVO₄ postsynthetic treatments and identifies important avenues of future inquiries.

The efficiency of solar fuels production requires consideration of both the photocurrent and the applied voltage bias. The role of photocurrent is apparent and scales linearly with the energy stored. Most oxide-based PEC devices require some externally applied voltage bias (E_{app}). Thus, the resulting fuel contains energy from both the external voltage source and absorbed light. The use of excessive bias voltage diminishes the balance of solar energy stored. The applied bias photon-to-current efficiency (ABPE) takes this important applied potential into account when expressing the efficiency of conversion from solar to chemical energy:[5,6]

$$ABPE(\%) = \left[\frac{(J_{photo})(mA\,cm^{-2}) \times (E_{rc} - E_{app})(V)}{P_{photo}(mW\,cm^{-2})} \right]_{AM1.5G} \times 100 \quad (1)$$

where J_{photo} is the measured photocurrent at a particular applied potential (E_{app}) and P_{photo} is the power density of AM 1.5G (100 mW cm^{-2}); E_{rc} corresponds to the cell potential of the redox couple, and 1.23 V_{RHE} corresponds to the standard cell potential for water splitting. (Other units may be appropriately used.) It is important to distinguish between the ABPE calculated with a 2-electrode configuration (E_{app} is between the working and counter electrodes) for overall water-splitting versus the ABPE calculated with a 3-electrode configuration (E_{app} is between the working and reference electrodes). The ABPE values in Figure 1b were
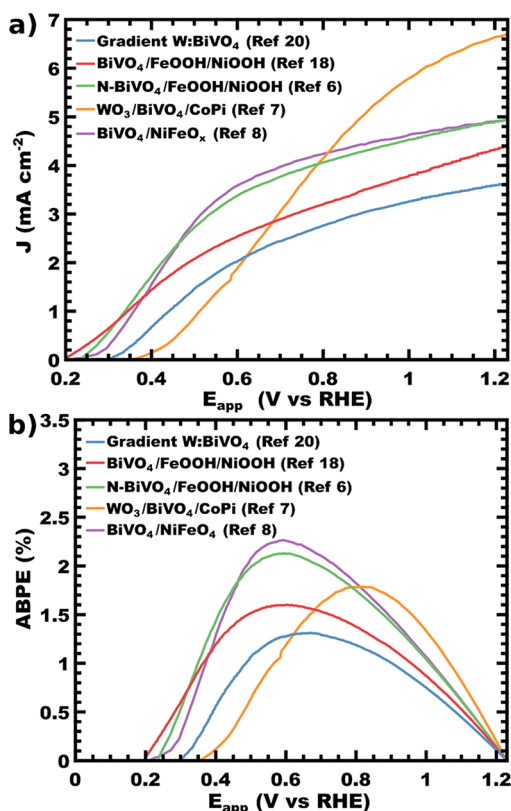
Figure 1. (a) $J-V$ characteristics of BiVO$_4$ photoanodes and (b) applied bias photocurrent conversion efficiencies of high-performing BiVO$_4$-based photoanodes. All data were obtained with a 3-electrode configuration to exclude variable counter electrode contributions.

calculated from 3-electrode data to provide a level comparison between samples because 3-electrode data is the most readily available in publications. Photocurrents as high as 6.7 mA cm^{-2} (~90% of the theoretical limit) have been reported for BiVO$_4$ with E_{app} = 1.23 V_{RHE};[7] however, operation at this voltage corresponds to an ABPE of 0% (Figure 1a). (Data were extracted from published figures using ScanIt 2.0 software.) Including both photocurrent and applied voltage shows maximum demonstrated ABPE values of 2.2−2.3% for BiVO$_4$ (Figure 1b; 0.6 V_{RHE}, 3.2−3.4 mA cm^{-2}).[6,8] A simple theoretical upper limit of 6.4−7.7% ABPE for water splitting may be estimated by considering the theoretical photocurrent limit (6.2−7.5 mA cm^{-2} for a band gap of 2.5−2.4 eV, respectively) and band positions (neglecting HER and OER overpotential losses, i.e., photocurrent saturation at 0.2 V_{RHE} with 100% fill factor). Clearly, there remains much

room for ABPE improvement by focusing on improving low-bias-voltage operation. Design strategies should thus work to maximize both charge separation and charge injection of BiVO$_4$ with low applied bias voltage.

Overview of Photoelectrochemical Processes in BiVO$_4$. For any photoelectrode material, the overall PEC performance, measured by J_{photo}, is determined by the combination of several phenomena, including the charge separation efficiency, the charge injection efficiency, and light-harvesting efficiency (LHE), and can be expressed as in eq 2. Here, J_{abs} is the photon absorption rate expressed as a current density (determined from LHE and the illumination spectrum), and ϕ_{sep} and ϕ_{inj} are the charge separation and charge injection efficiencies, respectively (Figure 2a).[9,10]

$$J_{photo}(V) = J_{abs} \cdot \phi_{sep}(V) \cdot \phi_{inj}(V) \quad (2)$$

For pure BiVO$_4$, ϕ_{sep} is often limited by bulk recombination and trapping of charge carriers (Figure 2b),[11−16] whereas ϕ_{inj} is typically limited by slow water oxidation kinetics and surface recombination (Figure 2c), although these can effectively be mitigated with the addition of cocatalyst layers.[17−19] The efficiency of each step is dependent on physical and chemical processes within the bulk or at the surface of the material. The relative rates of water oxidation (k_{wo}) and recombination (k_{rec}) determine the charge injection efficiency ϕ_{inj} at the surface (assuming 100% faradaic efficiency) (eq 3).[17,19]

$$\phi_{inj}(V) = \frac{k_{wo}(V)}{k_{rec}(V) + k_{wo}(V)} \quad (3)$$

Charge separation is accomplished by a combination of drift from an external applied potential or from the internal potential from the space charge layer (SCL), as well as diffusive charge transport. For pristine (undoped) BiVO$_4$, the SCL width can be as high as 90 nm;[17] this would enhance ϕ_{sep} of very thin, < 90 nm, films. In contrast, thicker films (>200 nm) are needed to achieve reasonable LHE values, dimensions where ϕ_{sep} is considerably reduced because most carriers are produced outside of the SCL. This may be mitigated by enhancing the extent of band bending with gradient-doping.[20] Use of a large external bias voltage can enhance charge separation at the cost of significant loss of overall ABPE. The separation of charge carriers produced far from the SCL is limited by low carrier conductivity as well as recombination sites within the film or at the substrate−BiVO$_4$ interface.[11,13] Here, because BiVO$_4$ is normally operated with bias voltage, improvements to conductivity (product of mobility and carrier concentration) can improve charge separation.

Defining Synthetic versus Postsynthetic Modification. Synthetic strategies to improve the PEC properties of BiVO$_4$, such as nanostructuring films, designing heterostructures, applying oxygen evolution catalysts (OECs), adding dopants to BiVO$_4$, among others, have been developed and used to great effect, and were reviewed elsewhere.[3,21,22] Postsynthetic treatments have been concurrently developed and have enabled many of the highest photocurrents reported to date.[6−8] These treatments are applied after the synthesis of BiVO$_4$ and are based upon illumination, chemistry, electrochemistry, or combinations thereof. Postsynthetic treatments are intended to modify the defect chemistry of existing material rather than to deposit additional material. For this reason, treatments that deposit metallic elements are not considered postsynthetic treatments. For example, here we consider annealing BiVO$_4$ under H$_2$ or N$_2$ gases to be postsynthetic treatments, whereas the deposition of
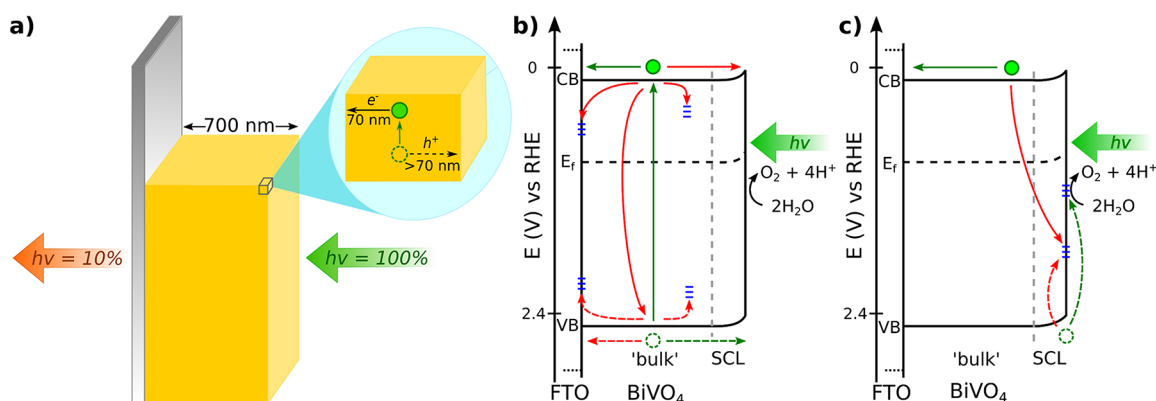
Figure 2. For solid films, there is a trade-off between light-harvesting efficiency and charge separation efficiency (a). Band diagrams of BiVO$_4$ showing stepwise processes toward water splitting with (b) light-harvesting and charge separation (ϕ_{sep}) followed by (c) charge injection (ϕ_{inj}). The green paths support water splitting, whereas the red paths are loss pathways.

passivation or catalytic layers (e.g., FeOOH, CoPi, etc.) is a synthetic treatment. Broadly, postsynthetic treatments affect ϕ_{sep}, ϕ_{inj}, or both to improve the overall ABPE performance of BiVO$_4$.

An electrochemical treatment of Mo:BiVO$_4$ was reported in 2011;[23] this was followed by H$_2$-annealed BiVO$_4$ in 2013 and subsequent follow-ups.[24−27] In 2015, N$_2$-annealed BiVO$_4$ was demonstrated to attain one of the highest ABPEs on record,[6] second only to a report on electrochemically treated catalyzed BiVO$_4$ in 2016.[8] Two illumination-dependent treatments, UV-curing and photocharging of BiVO$_4$, were published in 2015,[28,29] with later follow-up reports.[30,31] In 2016, a significantly accelerated PEC activation used a combination of light, electrolyte, and applied potential.[32]

The defect changes during postsynthetic treatments are sometimes subject to multiple equivocal interpretations as many of the proposed mechanisms are consistent with the often limited experimental data. For example, the addition of both hydrogen interstitials[30] and hydrogen antisite on oxygen[26] as well as both the addition[24] and removal[26] of oxygen vacancies have been supported by similar shifts in vanadium X-ray photoelectron spectroscopy (XPS) data; such contradictory defect chemistries clearly require additional investigation. Furthermore, multiple intrinsic (e.g., oxygen, bismuth, or vanadium vacancies ($v_O^{\bullet\bullet}$, v_{Bi}''', and v_V''''); interstitials (O_{int}'', $Bi_{int}^{\bullet\bullet\bullet}$, and $V_{int}^{\bullet\bullet\bullet\bullet\bullet}$); and antisites ($Bi_V''$ and $V_{Bi}^{\bullet\bullet}$)) and extrinsic (e.g., hydrogen interstitial, $H_{int}^{\bullet}$, or substitution, $H_O^{\bullet\bullet\bullet}$) defects are proposed to exist in BiVO$_4$, either directly after synthesis or after exposure to PEC conditions (i.e., illumination and electrolyte).[26,27,30] Additionally, defect clusters, e.g., double or triple vacancies like $v_{Bi}'''v_O^{\bullet\bullet}$, $v_{Bi}'''v_O^{\bullet\bullet}v_{Bi}'''$, or $v_{Br}'''v_{Bi}'''v_O^{\bullet\bullet}$, are also proposed to affect the catalytic activity of semiconductor photoelectrodes.[33] Differentiating between these numerous possible defect chemistries will require more detailed follow-up studies using experimental techniques that can probe local electronic environments and subsequently study charge carrier kinetics to elucidate defect activity (e.g., as trap, donor, and/or catalytic sites). Furthermore, the synthetic route dependence on subsequent postsynthetic behaviors is rarely considered; is it not reasonable that the native material defects should affect the results of a postsynthetic treatment?

The emergence of postsynthetic treatments highlights new opportunities to understand and improve photoelectrodes. Similar mechanisms may be of further utility as researchers turn more focus toward the development of novel multinary

> The emergence of postsynthetic treatments highlights new opportunities to understand and improve photoelectrodes.

metal oxide photoabsorbers where, like BiVO$_4$, there is a combinatorial expansion of the candidate point defect chemistries. Lastly, postsynthetic treatments also elucidate possible electrode changes under extended service and can provide new strategies to enable extended device performance. This Perspective will provide an overview of a variety of reported postsynthetic treatments and attempt to describe unifying features between treatments as well as paths forward toward a deeper understanding.

Postsynthetic Improvement of Charge Separation. Synthetic approaches to improve ϕ_{sep} are based on two main approaches: increasing the free carrier density by substituting V with higher-valent metals (e.g., Mo, W)[10,13,20,23,34−37] and limiting recombination at the back-interface by adding "hole-blocking layers," such as SnO$_2$ or WO$_3$, between BiVO$_4$ and the substrate.[7,11−13,38,39] Postsynthetic techniques have recently emerged with similarly significant improvements to charge separation.

Postsynthetic Removal of Recombination Sites. Bismuth vanadate photoelectrodes have been synthesized using numerous techniques including sol−gel,[10,40] spray pyrolysis,[11] electrodeposition and conversion,[8,18,41] magnetron sputter deposition,[37,42,43] chemical vapor deposition (CVD),[44] and atomic layer deposition (ALD),[32,45] where each method results in varying performance, partially due to the nature of the inherent defects. The combination of mobility and carrier lifetime results in a limited ~70 nm transport length of electrons within BiVO$_4$, with holes able to diffuse farther.[13] This characteristic is why numerous BiVO$_4$ publications report higher photocurrents with back-side illumination to minimize the transport distance for electrons.

Many of these synthetic techniques have been utilized to create high surface area architectures in an effort to enhance charge separation. The nanostructuring of pure BiVO$_4$ improves minority carrier (hole) transport to the surface,[8,18] whereas host−guest approaches are needed to improve electron transport to the substrate.[7,39,46−49] To date, the methods used for the production of BiVO$_4$ host−guest nanostructures have all utilized
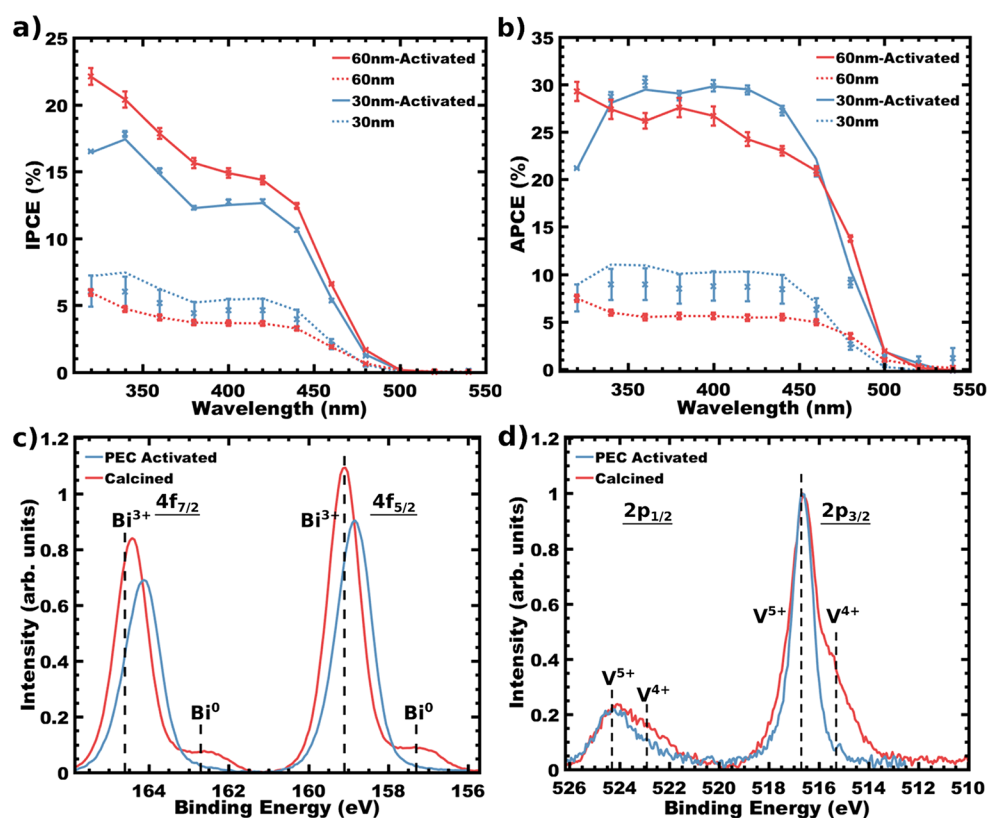
Figure 3. Effect of a postsynthetic PEC activation treatment on 30 and 60 nm films prepared by SF-ALD: (a) IPCE, (b) APCE, and XPS of (c) Bi 4f and (d) V 2p comparing as-made and activated SF-ALD BiVO$_4$. Reproduced with permission from ref 32. Copyright 2017 The Royal Society of Chemistry.

nonuniform depositions or cathodic electrodepositions that limit the use of hole-blocking layers at the BiVO$_4$−substrate interface.[7,39,46,47] Atomic layer deposition (ALD) stands out as a method to fabricate conformal BiVO$_4$ coatings within complex device architectures while retaining compatibility with hole-blocking layers and radial dopant profiles.[45] Surface functionalized ALD (SF-ALD) was recently shown to enable phase-pure scheelite BiVO$_4$.[32]

The ϕ_{sep} of SF-ALD BiVO$_4$ was remarkably sensitive to postsynthetic treatment. Postsynthetic enhancements were maximized with a treatment that involved exposing the sample to AM 1.5G simulated illumination while applying an external bias of 0.6 V$_{RHE}$ for 1 h. Corresponding to this treatment (PEC activation), film optical absorptance decreased, ϕ_{sep} increased, and both absorbed and incident photon-to-charge efficiencies increased (APCE and IPCE, respectively; Figure 3a), with an increase of APBE from 0.18 to 0.28% for 75 nm thick films in electrolyte with hole scavenger (sulfite, E_{rc} = 0.93 V$_{RHE}$ in eq 1).[32,50] Note that ϕ_{inj} is assumed to be unity in the presence of hole scavenger; no water oxidation data were presented. The simultaneous increase of transparency with photocurrent is counterintuitive given the relationship between LHE and photocurrent in eq 2. This effect is attributed to the removal of metallic defects during treatment (vide infra), which is expected to improve ϕ_{sep} by removing photoabsorbing trap sites, thus decreasing the overall optical absorption. The postsynthetic enhancements were shown to be stable for at least 17 h. During PEC activation, an oxidative photocurrent was observed to increase and plateau; this was attributed to the combined oxidation of hole scavenger and BiVO$_4$ defects. XPS (Figure 3b) analysis suggested that reduced metal defects in calcined SF-ALD

samples (Bi^0 and V^{4+}) were fully oxidized (Bi^{3+} and V^{5+}) following PEC activation. The ALD of bismuth titanates with the same Bi^{3+} precursor was previously shown to result in a mixture of Bi^{3+} and Bi^0,[51] highlighting the connection of synthetic route with point defect chemistries. Related postsynthetic treatments such as UV-curing and photocharging also involve illumination;[29,30] however, control experiments demonstrated that the applied bias with PEC activation leads to larger improvements to ϕ_{sep} and occurs much faster within 1 h. The ability of bismuth vanadate to self-heal may explain its label as a "defect tolerant" material.[13] More work is needed to establish the precise nature of the defects present in untreated BiVO$_4$ and to determine if any other phenomena are taking place; e.g., hydrogen or proton uptake or surface state alteration.[26,27,30]

Annealing BiVO$_4$ films in H$_2$ was found to increase the concentration of V^{4+} species while removing or passivating trap states.[24,26,27] H$_2$-annealing has been demonstrated to improve the onset potential and photocurrent of the photoelectrodes (93 mV shift to onset potential and increase to photocurrent from 1.23 to 1.43 mA cm^{-2} at 1.23 V$_{RHE}$ between as-grown and 290 °C H$_2$-annealed BiVO$_4$, respectively),[24,26] corresponding to an increase in APBE for sulfite oxidation from 0.18 to 0.27% between as made and H$_2$-annealed BiVO$_4$. Optimal annealing conditions were reported as 15 min at 290 °C under 1 atm of H$_2$.[26] H$_2$ annealing primarily improves ϕ_{sep}; however, a decrease in ϕ_{inj} was also reported,[27] possibly due to surface H affecting water oxidation kinetic activity.[27,52,53] Additionally, changes to the surface hydroxyl (−OH) concentration were reported;[25] such alterations were reported to affect ϕ_{inj} in BiVO$_4$.[28,29] This treatment was found to improve photocurrent regardless of synthetic procedure[27] and was helpful in improving the

photocurrent of other photoanode materials.[54−56] In the initial report,[24] density functional theory (DFT) calculations suggested that elemental H was occupying both interstitial and oxygen sites within the BiVO$_4$ lattice, with both types of defects expected to act as shallow donors. A follow-up report identified two local hydrogen environments by ^{1}H NMR spectroscopy that were attributed to interstitial hydrogen (H$_{int}$) and substitutional hydrogen (H$_O$).[26] Notably, H$_O$ also had a trace presence in as-made BiVO$_4$. This was further supported by a second follow-up report that quantitatively analyzed the loading of hydrogen into BiVO$_4$ by ^{15}N nuclear reaction analysis, finding about 5× the amount of hydrogen in annealed films (0.7 vs 0.14 at% for H-BiVO$_4$ and BiVO$_4$, respectively).[27] Initially, the partial reduction of V from 5+ to 4+ was attributed to the formation of oxygen vacancies, v$_O$.[24] However, subsequent investigations correlated H$_2$-annealing to a reduced photoluminescence (attributed to removal of v$_O$)[26] and increase in charge carrier lifetime, suggesting a decrease in trap concentration by the removal or passivation of traps (proposed to be interstitial V or V antisite on Bi, V$_{int}$, or V$_{Bi}$).[27] Follow-up reports also agree on the presence of one of the aforementioned hydrogen defects (H$_{int}$, bonded to a bridging O) and that increasing the v$_O$ content is not the source of improved ϕ_{sep}. There remains some question as to the nature of the trap states removed or passivated (e.g., v$_O$, V$_{int}$, or V$_{Bi}$).[26,27] Furthermore, there is disagreement as to the effect of H$_2$-annealing on charge carrier conductivity.[26,27] Considering that both v$_O$ and H$_O$ can yield the same XPS observation of partially reduced vanadium, follow-up studies on hydrogenated photo-electrode materials would benefit by parsing the multiple causal pathways with further measurements such as electron energy loss spectroscopy (EELS)[57−59] or X-ray absorption near edge structure (XANES)[60] to probe changes to local electronic environment caused by specific defect chemistries.

Postsynthetic Production of Free Carriers. Doping BiVO$_4$ with metals and nonmetals, commonly W and Mo, has been widely utilized to synthetically alter the carrier density and conductivity of BiVO$_4$-based photoanodes.[11,13,23,28,34−37,61] Recently, several postsynthetic techniques have been utilized to similarly increase free carrier density.[6,8,62] It has been suspected that V^{4+} plays a role in the native conductivity of BiVO$_4$ photoanodes,[63] typically attributed to the formation of O vacancies (v$_O$) as a shallow donor state.[64] Consequently, several postsynthetic treatments have related effects to conductivity and ABPE to alterations in V oxidation state.[8,24,62] However, recent work has shown that the mobility of charge carriers in BiVO$_4$ is not improved by increasing v$_O$ concentration,[26,27] suggesting that an alternative mechanism may be present.

To achieve one of the highest reported ABPEs, researchers activated their electrodes with a simple cyclic voltammetry treatment in alkaline media prior to depositing the catalytic Ni-borate layer.[8] This treatment (five cycles of voltammetric scans from 0 to 1 V$_{RHE}$ at 40 mV s^{-1}) was suggested to involve the reversible redox between V^{5+} and V^{4+}. Improvements to ϕ_{sep} following this treatment were attributed to an improved (lower gradient) distribution of V^{4+} near the surface of the film.[8] The authors noted that others had observed a 5 nm "reduction shell" at the surface of BiVO$_4$; however, those observations were on commercial powders that had not carried out PEC, and the scanning transmission electron microscopy (STEM) imaging may have itself induced changes.[58] Within this reduction shell, vanadium primarily exists in the 4+ state, compared to the 5+ state of bulk V, producing a n$^+$−n homojunction that is deleterious to charge separation.[8,58] It was also noted that

onset potential was affected by vanadium redox changes. An anodic shift to onset potential was observed with starting potentials of 0.05−0.25 V$_{RHE}$ in current−potential scans, indicating overly reduced V^{4+} produces charge recombination sites.[8] An alternative mechanism for film activation could involve the incorporation of hydrogen defects (H$_{int}$ or H$_o$, for example), which would also reduce vanadium while introducing shallow donors; further measurements could clarify the changes to defect chemistry caused by such treatments. Calculation of the relative ABPE enhancement would require electrochemical data from the as-made sample.[8]

Doping BiVO$_4$ with N$_2$ (N-BiVO$_4$) was also shown to primarily improve photocurrent and ϕ_{sep}.[6] Charge injection efficiency was calculated to slightly increase as well. This treatment was reported to incorporate N in the lattice, accompanied by the generation of v$_O$. Using Kröger−Vink notation, the proposed reaction was[6]

$$3O_O^x + N_2(g) \rightarrow 2N_O' + v_O^{\bullet\bullet} + 1.5O_2(g) \tag{4}$$
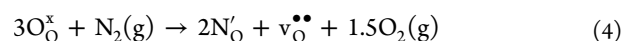
where O$_O^x$ denotes oxygen on an oxygen site, N$_O'$ nitrogen on an oxygen site, and v$_O^{\bullet\bullet}$ an oxygen vacancy. N-BiVO$_4$ was achieved by annealing under N$_2$ at 350 °C for 2 h. N-BiVO$_4$ resulted in a reduced band gap (∼0.2 eV less) compared to untreated BiVO$_4$ by increasing the VB maximum, as suggested by DFT calculations and IPCE measurements. Whereas v$_O$ are proposed by some to yield localized trap states in BiVO$_4$,[6,26] the v$_O$ production in N-BiVO$_4$ was also accompanied by a shift of the valence band toward the conduction band, enhancing activation of v$_O$ as donor states. The charge mobility increased by 25%, corresponding to an improvement in ϕ_{sep} from 88 to 94% at 1.0 V$_{RHE}$. The concomitant reduction of band gap notably also improved optical absorbance.[6] The authors noted that the changes in the XPS spectrum were not suggestive of changes to the Bi nor V oxidation states, unlike several other postsynthetic treatments discussed thus far. Overall, N-BiVO$_4$ produced one of the highest ABPEs reported to date (2.16%); in comparison, untreated BiVO$_4$ samples demonstrated an ABPE of 1.63%. Additionally, the photocurrent for sulfite oxidation was stable for 50 h without decay,[6] and water oxidation photocurrents decayed after 30 h because of film degradation (perhaps caused by the use of a phosphate buffer).[6,8,65] Further investigation into the defect chemistry specific to BiVO$_4$ synthesized in this manner (i.e., electrodeposition and conversion) could be particularly insightful, given the exceptionally high performance (APBE) of this and similar reports (for example, refs 8 and 18).

Although the partial reduction of vanadium species is often correlated with improved PEC properties (e.g., ϕ_{sep} or ϕ_{inj}), the direct (electro)chemical reduction of BiVO$_4$ is not as effective.[62] For example, BiVO$_4$ was reduced electrochemically for 3 min at ca. −0.3 V$_{RHE}$ followed by chemical reduction in 0.1 M NaBH$_4$ for 3 min which enhanced the photocurrent from 0.5 to 1.4 mA cm^{-2} at 1.2 V$_{RHE}$ and was ascribed to an enhanced free-carrier density from the production of v$_O$ and the associated reduced vanadium oxidation states, as evidenced by XPS.[62] ABPE increased from 0.04 to 0.16% following this combined treatment. However, the benefits of this treatment were stable for only 40 min before the photocurrent began to decay significantly, returning to the initial (untreated) photocurrent after 75 min. The instability of this treatment might be due to the over-reduction of BiVO$_4$,[26] possibly resulting in the reoxidation of species within the electrode. Additionally, more mild reducing treatments (e.g., annealing in Ar to induce v$_O$ formation or less

aggressive electrochemical treatment) have resulted in little to no change to $BiVO_4$ water oxidation performance.[23,27]

Briefly we note that the conductivity of $BiVO_4$ may also be enhanced thermally or by significantly increasing photon flux. The low minority carrier mobility in $BiVO_4$ is caused by localization of the carriers as small polarons.[66] A modest temperature increase from 10 to 42 °C was shown to activate minority carrier hopping in $BiVO_4$ and significantly enhance the PEC activity from 1.8 to 4.0 mA/cm^2 at 1.0 V_{RHE}.[36] Similarly, increasing the concentration of incident photons (from $\sim10^{18}$ photons cm^{-2} s^{-1} for AM 1.5 to $\sim10^{24}-10^{28}$ photons cm^{-2} s^{-1}) can overcome trapping mechanisms for both charge carriers and significantly enhance mobility.[13,15,16,27]

Summary. Conventional methods of improving ϕ_{sep} in $BiVO_4$-based photoanodes have primarily been confined to heterometal dopants and hole-blocking layers.[11,34,39] Postsynthetic techniques that have recently emerged can supplement or replace synthetic approaches by removing common and/or synthesis-specific bulk defects and increasing the free carrier density.[6,8,24,26,27,32] The development of these postsynthetic

> The development of these postsynthetic techniques continues to improve the understanding of $BiVO_4$ defect chemistry and highlights the differences between various synthetic methods.

techniques continues to improve the understanding of $BiVO_4$ defect chemistry and highlights the differences between various synthetic methods.[26,27,32]

It is important to note that two of the techniques discussed produced stable improvements through mild (photo)-electrochemical treatments.[8,32] One may expect that these treatments affect only the near-surface; however, the improvements to ϕ_{sep} suggest that bulk changes may be occurring, for example, intercalation of hydrogen. Further data are needed to better understand these changes.

Postsynthetic Improvement of Charge Injection at the Surface. Postsynthetic treatments have been developed to modify the surface and near-surface regions of $BiVO_4$-based electrodes. As described briefly above, the ϕ_{inj} suffers from slow water oxidation kinetics, which causes an accumulation of holes within the SCL, particularly at BiO_8 polyhedra.[67] This accumulation makes the back-recombination of holes and electrons kinetically viable.[17] Recombination can also occur at surface defects at the $BiVO_4$–electrolyte interface.[23,35,68] Furthermore, the buildup of holes within the SCL and near the surface of $BiVO_4$-based photoanodes was linked to photocorrosion,[1,3] in particular when immersed in alkaline electrolytes.[65,69] Clearly, the best strategies to improve ϕ_{inj} and prevent electrode degradation should involve either increasing the rate of water oxidation or decreasing the rate of near-surface recombination (eq 3). Commonly, layers of additional materials as protective layers or catalysts, e.g., amorphous TiO_2,[35,38,69] CoPi,[10,12,70] $NiOOH$,[6,18] etc.,[8,68,69,71-73] are used to block native defects, store holes to mitigate side reactions, or catalyze the water oxidation reaction; however, simple postsynthetic modifications have also been used to mitigate surface defects.[23,29,30,68]

Removal of Surface Recombination Sites. Surface recombination sites can be removed or blocked by simple postsynthetic

treatments in both doped and pristine $BiVO_4$. These treatments provide simple routes to decrease k_{rec} and improve ϕ_{inj}, as described in eq 3. Simulations of $BiVO_4$ surfaces suggest that hole localization and subsequent recombination at the electrode–electrolyte interface is caused by native crystal distortions,[67] whereas experimental evidence supports a second recombination mechanism via segregated surface species.[23]

Ion segregation, or enrichment of a material constituent, at the surface of photoelectrodes has been known to form recombination centers.[23,74] In the case of Mo-doped $BiVO_4$ (Mo:$BiVO_4$), Mo^{6+} aggregates at the surface were dissolved by an electrochemical treatment of 30 cyclic voltammetry scans from −0.3 to 1.16 V_{RHE}, causing the photocurrent at ~1.2 V_{RHE} to approximately double when illuminated from the front of the photoelectrode, based on XPS and PEC characterization, corresponding to an increase in ABPE from 0.09 to 0.24%. Comparatively, nondoped $BiVO_4$ electrodes showed no effect on photocurrent following the same electrochemical treatment, suggesting that the untreated Mo^{6+} locations are recombination sites at the semiconductor/electrolyte interface.[23] Additionally, Mott–Schottky analysis suggested that bulk properties (e.g., carrier concentration) were not altered by the treatment; i.e., only ϕ_{inj} was affected.[23] Interestingly, a Bi-rich surface layer was observed following the electrochemical treatment, suggesting that V was also dissolved from the surface. The effect on photocurrent or stability caused by dissolving V from the surface or the enrichment of Bi at the surface was not reported,[23] though it should be noted that Bi-enriched $BiVO_4$ surfaces were previously shown to improve photocurrent stability.[75] It should also be noted that while this treatment and the EC/chemical treatment discussed in the previous section[62] both apply cathodic potentials to reduce electrode material, the potential discussed here was applied only for a brief time before sweeping to higher (oxidizing) voltages, compared to holding −0.3 V_{RHE} for 3 min.[23,62] For this treatment, cathodic potentials (versus V^{4+}/V^{5+}, $E_{app} < \sim0.1$ V_{RHE})[8] are applied for only ~6.5 s per scan before the sweep becomes anodic (~36.5 s for 0.1 < V_{RHE} < 1.2). It would seem that any reduction of V or other species within these $BiVO_4$ films is reversed by the oxidation involved in each sweep, with the exception of surface Mo^{6+} which is apparently dissolved irreversibly into solution. Additional differing results between this treatment and the previously discussed EC scanning treatment[8] can be at least partially explained by the electrolytes used (sodium sulfate at pH 6.5 versus potassium borate at pH 9.4), as pH is known to strongly affect postsynthetic treatment.[30] However, direct experimental comparison would be needed to confirm these hypotheses. This electrochemical treatment was found to be stable after storing treated electrodes in air or vacuum for 12 h.[23]

While not strictly a postsynthetic treatment by our definition, etching of an NiO_x catalytic layer on $BiVO_4$ was proposed to block recombination sites ascribed to BiO_8 polyhedra at the electrode surface.[67,68] Computational modeling suggested that lattice distortions within the first ~2 nm of $BiVO_4$ surfaces create an environment favorable for hole trapping.[67] Bi^{3+} surface sites were reportedly blocked by the selective etching of nickel borate surface layers in a potassium phosphate solution.[68] The etching procedure exposed VO_4 sites while the remaining, noncatalytic NiO_x was primarily located on BiO_8 sites. The resulting films exhibited a significant improvement to ϕ_{inj}, improving the stable photocurrent at 1.23 V_{RHE} from 0.34 to 1.09 mA cm^{-2}[68] and improving ABPE to 0.39% from 0.07 and 0.15% for untreated and NiO_x catalyzed films, respectively. A small improvement of
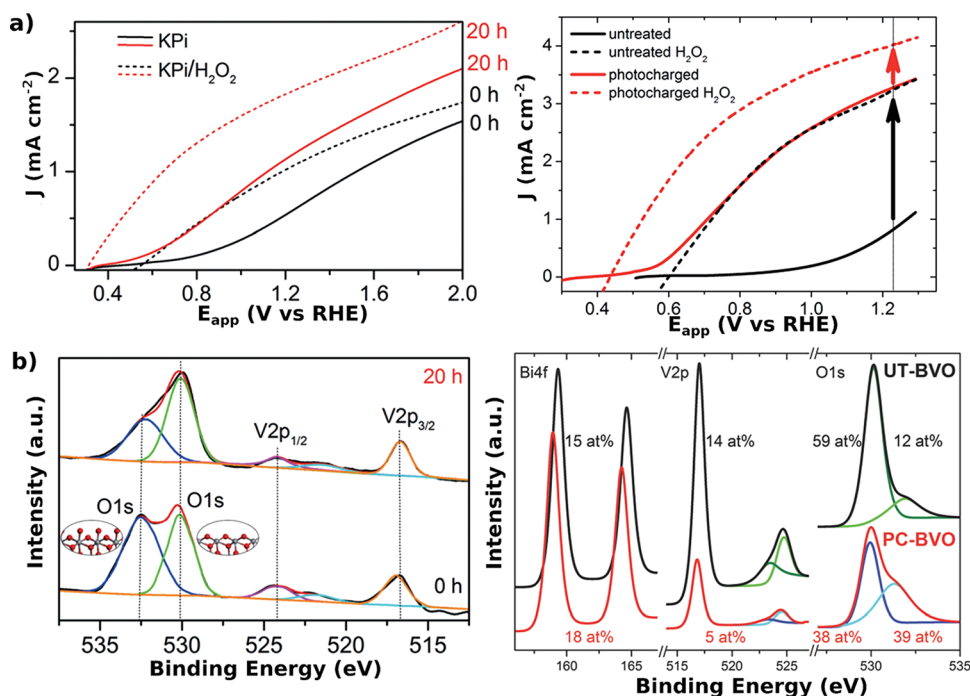
Figure 4. (a) (left) Photocurrent densities of $BiVO_4$ photoanodes, before and after exposure to 20 h of UV curing, in KPi buffered solutions (solid) and after the addition of 0.1 m H_2O_2 (dashed), at pH 7; (right) $J−V$ scans of 200 nm thick $BiVO_4$ under back-side AM 1.5 illumination, in 0.1 M K-Pi buffer (pH 7.2). Arrows denote catalytic limitations for untreated (black) and photocharged (red) material. (b) (left) O 1s and V 2p peaks of $BiVO_4$ with 0 h (black) and 20 h (red) UV curing in XPS spectra normalized to V $2p_{3/2}$ signal. The inset images represent the possible structures of crystalline oxygen (530.3 eV) and oxygen-based defect sites (532.3 eV) on the surface. The red spheres represent O atoms, and gray spheres represent V atoms. (right) XPS spectra of $BiVO_4$ photoanodes before and after photocharging in 0.1 M PBA buffer, pH 10, under AM 1.5G simulated illumination. Left-hand images in panels a and b are reproduced with permission from ref 28. Copyright 2016 Wiley-VCH Verlag GmbH & Co. KGaA. Right-hand images in panels a and b are reproduced with permission from refs 29 and 30, respectively. Copyright 2016 and 2017 The Royal Society of Chemistry.

ϕ_{sep} for both catalytic and etched $NiO_x/BiVO_4$ samples over bare $BiVO_4$ can be observed in photocurrent data with hole scavenger (sulfite) present.[68] This work emphasizes the crucial role of surface termination, particularly with multinary materials. Future work on this treatment could be directed toward improving the treatment route, e.g., by directing the passivating material to the recombination sites initially and removing the need to etch, and investigating the surface chemistry of $BiVO_4$ (for example, the role of different exposed metal sites and the passivation mechanism of NiO_x sites).

These postsynthetic techniques target both the electrode– electrolyte interface and improving ϕ_{inj} by removing or blocking surface recombination sites and represent facile approaches to enhance the performance of both doped and pristine $BiVO_4$ photoanodes.[23,68] These diverse results highlight that there is not a specific ideal surface termination because both Bi and V surface-rich terminations were observed with improved charge injection, depending on the particular report.

Near-Surface Doping and Surface State Alteration. In the near-surface regime (i.e., 2−10 nm),[67] partial reduction of V through photochemical treatment has been associated with improved ϕ_{sep} and ϕ_{inj}.[28−30] Photochemical treatments have been demonstrated with both ultraviolet and visible light, and the resulting effects can be achieved either in or out of electrolyte, depending on the report.[28−30] Soaking $BiVO_4$ in $AgNO_3$ can also improve ϕ_{inj} significantly.[75]

Relatively early in the PEC research on $BiVO_4$, it was noticed that the photocurrent in pristine $BiVO_4$ decayed as much as 50% within 30 min, yet the photocurrent could be partially restored by

cyclic voltammetry or storing the electrodes in the dark for 24 h.[75] Based on the existing knowledge of photoelectrode surface modifications, this work exposed $BiVO_4$ to a number of metal salts (0.01 M, 12 h) to adsorb metal ions into $BiVO_4$. Of the different salts tested, $AgNO_3$ solutions showed the most improvement in photocurrent. Following $AgNO_3$ treatment, ϕ_{inj} was improved to near-unity and ϕ_{sep} was slightly improved at high potentials (1.15−1.55 V_{RHE}); APBE was improved from 0.06 to 0.21%. (Photocurrent was measured using an unfiltered Xe lamp with ca. 2.6 × AM 1.5G intensity. Therefore, 260 mW cm^{-2} was assumed as the illumination power.) $BiVO_4$ treated with $AgNO_3$ demonstrated a stable photocurrent (1 h) plateauing at nearly twice the saturation photocurrent of untreated $BiVO_4$. Following an XPS analysis on the effect of 1 h of photoreaction (e.g., PEC water splitting) on treated and untreated $BiVO_4$, it was found that V dissolved from the surface of both treated and untreated samples; however, the surface of treated $BiVO_4$ was capped by a Bi-rich layer. The surface of $AgNO_3$ treated $BiVO_4$ was etched following photoreaction; beneath the surface, Bi and V were found to be stoichiometrically matched even with 1.8 at% Ag^+ present, and Bi was found to be both in the normal Bi^{3+} and reduced Bi^0 oxidation states; here it should be noted that by incorporating metal species to $BiVO_4$, this treatment is not strictly a postsynthetic treatment. The researchers attributed the improved photocurrent and stability to both the protective Bi-rich surface layer and the Ag^+ ion exchange layer formed at the surface of $AgNO_3$-treated $BiVO_4$.[75] Additionally, it was hypothesized that the addition of Ag^+ to the near-surface region of $BiVO_4$ would raise the VB maximum

within this spatial region,[3,76] thus narrowing the band gap and improving charge separation as well as absorption. Further evidence would be needed to support this hypothesis.

For W-doped BiVO$_4$ (W:BiVO$_4$), curing electrodes in air with UV light ($\sim$10 mW cm^{-2}, 20 h) significantly enhanced both ϕ_{sep} and ϕ_{inj} (Figure 4a).[28] The improvement of ϕ_{sep} was demonstrated by comparing photocurrents before and after treatment in the presence of a hole scavenger (H$_2$O$_2$). Evidence of ϕ_{inj} improvement was shown by the change in photovoltage from 0.17 to 0.41 V,[28,77] as well as the comparison of water oxidation photocurrents in relation to the photocurrents in a hole scavenger. UV-cured W:BiVO$_4$ films showed an improved ABPE for water oxidation (0.20%) over untreated samples (0.07%). The improvements of ϕ_{inj} were attributed to a change in the ratio of dangling to bridging (oxy)hydroxyl group surface groups at the electrolyte−electrode interface, where the amount of bridging O was increased following UV-curing. Alterations to film crystallinity and texture were also observed and would be expected to affect ϕ_{sep}.[28] Further analysis on the effects of this treatment (e.g., defect chemistry, carrier kinetics) in relation to other photo(electro)chemical treatments could offer important insights into the differences between pristine and doped BiVO$_4$.

A separate light-based treatment was demonstrated to address the limitations of BiVO$_4$, denoted as "photocharging",[29,30] which uses long-time exposure of the BiVO$_4$ photoanodes to AM 1.5G illumination under open-circuit conditions in a cell filled with electrolyte. Photocharging leads to greatly enhanced photocurrent, a strong cathodic shift of the photocurrent onset, and improved J−V fill factor (Figure 4b). The photocharging-driven activation of BiVO$_4$ photoanodes is facilitated especially under alkaline conditions, with slightly alkaline electrolyte (pH 10) showing the greatest performance enhancements and slightly acidic media (pH 4) showing no effect following photocharging;[30] photocharged samples in pH 10 buffer were found to have an ABPE of 1.67%, versus an ABPE of 0.16% for untreated films. It is worth noting here that not all basic media are appropriate for BiVO$_4$-based electrodes; phosphate buffers especially are known to etch BiVO$_4$ to the detriment of film performance and stability.[8,65] The combination of requirements, principally alkaline electrolyte and visible light illumination, led to the conclusion that photogenerated holes (h$^\bullet$) and hydroxide ions cause two main effects: (i) hydrogenation of the near-surface region, proposed as the formation of interstitial positively charged defects (H$_{int}^\bullet$) and resulting in V^{4+} and oxygen vacancies (v$_O^{\bullet\bullet}$), and (ii) saturation of the electrode surface with hydroxyl groups, which act as intermediates in the OER.[30] The proposed defect chemistry reaction, described using Kröger−Vink notation and shown in eq 5, presents self-doping of the V$_2$O$_5$ sublattice with reduced VO$_2$ species, in alkaline conditions (OH$^-$) and under illumination (h$^\bullet$). Here, care should be taken to distinguish between a vanadium in vanadium site (V$_V'$) and a vacant oxygen site (v$_O^{\bullet\bullet}$). Furthermore, the (O$_O^x$) denotes the oxygen atoms occupying the regular oxygen sites.

$$2VO_2 + OH^- + 2h^\bullet$$
$$\xrightarrow{V_2O_5} 2V_V' + 4O_O^x + v_O^{\bullet\bullet} + H_{int}^\bullet + 0.5O_2(g) \quad (5)$$
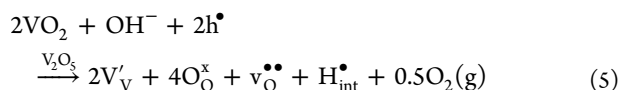
These surface and near-surface alterations result in a record high photocurrent for undoped and uncatalyzed BiVO$_4$ of 4.3 mA cm^{-2} at 1.23 V$_{RHE}$, an onset potential of 0.25 V$_{RHE}$ corresponding to a doubling of the photovoltage, improved ϕ_{inj} and ϕ_{sep}, and near-unity internal quantum efficiency.[29,30] Electrochemical impedance spectroscopy (EIS) characterization

suggests that photocharging leads to the formation of a surface capacitive layer, which has the ability to accumulate holes and hence reduces the surface recombination. The formation of this capacitive layer involves the increase of hydroxyl groups at the surface and the partial reduction of vanadium 5+ to 4+, as supported by X-ray photoelectron spectroscopy and X-ray absorption spectroscopy (XAS) measurements,[30] and more recently by intensity modulated photocurrent spectroscopy (IMPS).[31] IMPS results further elucidated that ϕ_{inj} improvements (caused by the aforementioned surface state changes) increased charge transfer while decreasing recombination (k$_{WO}$ and k$_{rec}$ in eq 3, respectively).[31]

Contrary to the UV-curing study, which can enhance performance even when illuminated in air, photocharging could be performed only in an aqueous solution. While the surface states were observed to change following both treatments, the trends were opposite; i.e., increasing amount of dangling −OH surface sites in case of photocharging in an electrolyte and passivation of −OH in case of UV-curing in air (Figure 4b).[28,30] These differences between UV-cured W:BiVO$_4$ and photocharged BiVO$_4$ might be caused either by the differences in deposition method (sol−gel spin coating vs spray pyrolysis, respectively) which can cause different intrinsic surface or bulk defects[29] or by the addition of W to BiVO$_4$ in the UV-curing case which is known to form extrinsic trap states.[13,27] As noted previously, doping BiVO$_4$ can cause significant alterations to the surface of BiVO$_4$;[23] furthermore, doping BiVO$_4$ with W is known to form additional trap states (versus pristine BiVO$_4$), adversely affecting charge carrier mobilities and lifetimes.[13] More work is needed to confirm either of these hypotheses. Notably, the mechanism proposed for photocharging is very similar to that for H$_2$-annealed BiVO$_4$ and the role of hydrogen in BiVO$_4$, as discussed in the previous section.[26] Both treatments, H$_2$ annealing and photocharging, are proposed to introduce hydrogen defects (H$_O$, H$_{int}$) and v$_O$ as well as alter the surface states at the semiconductor−electrolyte interface. Both treatments have also been shown to improve ϕ_{sep} and increase the concentration of surface dangling −OH groups,[25,29] which were shown to improve ϕ_{inj} in photocharged samples.[30] In addition to the treatment conditions, the most significant difference between the electrodes is the localization of vanadium reduction to the near-surface (top 5−10 nm, based on XPS, XAS, and XANES results) of photocharged BiVO$_4$ compared to no reported localization in H$_2$-annealed BiVO$_4$. Similarities also exist between the photocharging treatment and some of the (photo)electrochemical treatments discussed in the previous section.[8,29,30,32] All of these treatments take place, optimally, in alkaline media and are accompanied by changes in the V oxidation state for an overall enhancement of photocurrent and improved onset potential. Indeed, the photocharging effect works best in alkaline media and not at all in acidic media.[30] Additionally, the initial report on photocharged BiVO$_4$ indicated that the treatment was reversible (i.e., unstable) when stored in the dark overnight in buffer;[29] however, EC-treated BiVO$_4$ was reported to be stable over extended measurements (10 h PEC, 10 days in borate electrolyte), perhaps owing to the deposition of a catalytic layer following the electrochemical treatment.[8]

These similarities point toward a relationship between three effective postsynthetic treatments for improving the PEC efficiency of BiVO$_4$, where H$_2$ annealing, photocharging, and electrochemical treatments achieve similar results based on possibly related underlying mechanisms.[8,26,27,30,32] Further data are needed to develop a deeper understanding and to find the

most effective treatments for further performance gains. Bringing new measurement techniques to bare on BiVO$_4$ will certainly help illuminate changes.[78−80]

Summary. Postsynthetic treatments offer powerful ways of removing a variety of surface recombination sites and improving (near)-surface kinetic properties of BiVO$_4$-based photoanodes.

> Importantly, the type of defect present (and therefore the synthetic method utilized) has a significant impact on the effectiveness of a given postsynthetic technique.

Importantly, the type of defect present (and therefore the synthetic method utilized) has a significant impact on the effectiveness of a given postsynthetic technique. For example, two similar treatments, UV curing and photocharging, are not interchangeable and seem to have opposite effects on different BiVO$_4$-based electrodes.[30] Likewise, two seemingly disparate treatments, PEC activation (oxidation) and electrochemical cycling, both improve electrodes similarly, presumably because the initial-state after synthesis has different native defects.[23,32] Therefore, as research on BiVO$_4$ electrodes continues, it is important to carefully characterize the types and location of defects present within BiVO$_4$ before and after treatments. This is especially important when comparing different synthetic routes but is equally relevant for the same synthesis where small changes to instrumentation can produce significantly different materials.[27]

Theoretical Limits. Enhanced theoretical models[81] based on the detailed balance concept[82] predict fundamental prospects of solar water-splitting devices and enable precise guidance for their development.[83] These models include fundamentally inevitable losses such as radiative recombination, thermalization, and transmission. However, oxide materials with highly nonideal semiconductor properties, such as BiVO$_4$, still represent significant challenges for both theoretical prediction and experimental implementation. Figure 5 compares the idealized optoelectronic performance limit for BiVO$_4$ (black line, in a hypothetical PV configuration) with present day record current−voltage characteristics (red and blue lines, PEC configuration, see
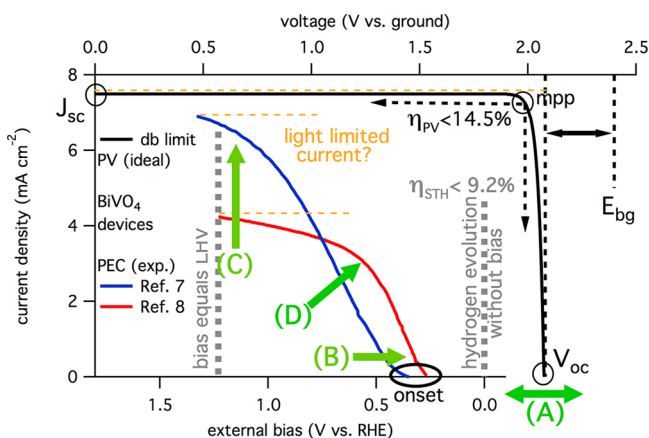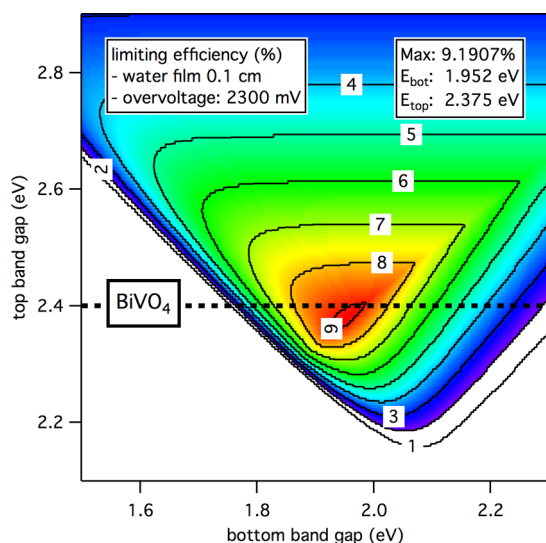
also Figure 1). The theoretical calculation (black line, Figure 5) assumes idealized material by neglect of nonradiative recombination, of lattice imperfections, and of system losses (including catalysis, band offsets, resistances, etc.) that largely diminish the performance of experimental BiVO$_4$ PEC devices. Fundamentally, its 2.4 eV band gap (E_{bg}) enables BiVO$_4$ to provide up to 2.1 V open-circuit voltage (V_{oc}) and 14.5% PV efficiency at a load of about 1.95 V (maximum power point, mpp). In the light of more than 700 mV sacrificial overvoltage (in excess of the thermodynamic water-splitting potential of 1.23 V), even bias-free PEC operation of a single-junction absorber may appear conceivable. However, a single-junction approach has not been achieved in practice because of major material deficiencies (recombination and poor band alignment) demanding a much higher overvoltage budget.

Experimental PEC performance of BiVO$_4$ (Figures 1 and 5) lags far behind that ideal, but at least positive net energy contributions (up to ∼2% APBE, see above)[6,8] have been realized. Present and future development deals with three major bottlenecks restricting solar-to-hydrogen (STH) energy conversion with BiVO$_4$: (i) nonradiative recombination, (ii) unfavorable band alignment, and (iii) an excessively large band gap energy. Engineering solutions such as host−guest architectures[7,39,49] decouple the mismatch of diffusion and absorption lengths enabling impressive photocurrents (Figure 5C). (We cannot exclude a certain level of overestimation in literature data,[86] but the significance of the achievements remains obvious.) Gradient doping improves charge carrier extraction[20] and thus effectively further suppresses the impact of nonradiative recombination events toward a more rectangular I−V characteristic (Figure 5D). Both concepts also promise minor improvements of the photocurrent onset potential (Figure 5C) but are limited by the intrinsically nonideal band alignment of BiVO$_4$ to the water oxidation−reduction potentials.

A priori, the transfer between absolute PV (upper axis) and relative PEC (lower axis) potential metrics (Figure 5A) remains unclear. Despite its high band gap and theoretical voltage prospects, BiVO$_4$ is considered incapable of driving unbiased water splitting because its band edges do not straddle both water-splitting half-reaction potentials.[84] However, appropriate engineering solutions such as surface modification with dipoles[85] or a buried p−n junction[83] may lessen or even resolve the misalignment. Tandem operation represents a more practical solution already demonstrated today.[20,86,87] Utilization of inevitable transmission losses (photons <2.4 eV) by a subsequently absorbing bottom PV structure may provide plenty additional (built-in) bias voltage. Figure 6 maps detailed balance tandem STH efficiency limits over both top and bottom absorber band gaps. Optimum structures may tolerate up to 2.3 V of overvoltage loss before severely restricting the performance prospects. The popular concept of combining BiVO$_4$ with multiple bottom junctions accommodates even higher losses.[20,86,87] Achieved performance gains indirectly demonstrate insufficient material quality of concurrent BiVO$_4$, where its I−V characteristics virtually never saturate to a light-limited photocurrent regime with low applied bias. Engineering concepts promise to combine more ideal performance with better photocurrent onset.

Summary and Future Outlook. Bismuth vanadate is a well-studied and interesting material for use in solar-assisted water splitting. Recently, a variety of postsynthetic modifications have emerged to improve the ABPE performance of BiVO$_4$. Postsynthetic treatments have provided insights into BiVO$_4$

Figure 5. Comparison of I−V characteristics of experimental BiVO$_4$ PEC devices (blue/red, bottom axis) relative to the theoretical detailed balance limit for BiVO$_4$ photovoltaics (black, top axis).

Figure 6. Detailed balance contour plots of the fundamental solar-to-hydrogen conversion efficiency limit for dual-junction water-splitting devices over the band gap energies of top and bottom absorber material for thin (1 mm) illumination length through the electrolyte and high (2300 mV) overvoltage loss.

defect chemistry at the surface and within the bulk of the material, yielding significant enhancements to charge injection and charge separation, respectively. Importantly, it has become apparent that probing the oxidation states by XPS alone cannot distinguish between the multiple posited changes to defect chemistries. For example, thermal hydrogenation,[24,26,27] proton intercalation,[29,30] production of oxygen vacancies,[6,24,29,30] and electrochemical reduction[8,62] all are expected to yield reduced vanadium states. XPS measurements of vanadium oxidation states alone are not sufficient to distinguish between these various defect mechanisms. New insights will be drawn from future studies that attempt to parse these multiple causal pathways in the presently reported observations. Techniques to probe local electronic environments, e.g., solid-state NMR (^{1}H, [51]V, and [209]Bi),[26,88−90] Raman and IR spectroscopy,[88,91] electron energy loss spectroscopy (EELS),[57−59] STEM,[58,92] and X-ray absorption near-edge structure (XANES),[60] could be used in conjunction with computational methodologies to identify changes to specific defect chemistries. Here, inelastic X-ray techniques have yielded recent insights into changes at the BiVO$_4$−electrolyte interface[78,80] and to electronic structure with changing defect chemistry.[4,79,93,94] Once the defects are identified with specificity, then techniques that probe charge carrier dynamics (such as transient diffuse reflectance and time-resolved conductivity)[16,27] or trap states (such as photo-luminescence)[26] could provide valuable insights into the role of those defects sites (e.g., catalytic site, trap site, and/or donor). Beyond immediate performance, postsynthetic treatments may also elucidate possible electrode changes under extended service and provide new strategies to enable extended device performance, furthering the development of commercial PEC water-splitting devices.

■ AUTHOR INFORMATION

ORCID ⓘ
Benjamin Lamm: 0000-0003-4041-7786
Wilson A. Smith: 0000-0001-7757-5281
Morgan Stefik: 0000-0002-2645-7442

Author Contributions
[⊥]B.L. and B.J.T. contributed equally to this work.

Notes
The authors declare no competing financial interest.

Biographies
Benjamin Lamm is a Ph.D. candidate at the University of South Carolina. He earned his BS (2014) in chemistry from Illinois Wesleyan University before joining Dr. Stefik's research group later that year. His research interests include photoelectrochemistry for solar energy conversion and nanomaterial architecture engineering (www.stefikgroup.com).

Bartek J. Trześniewski received his BSc and MSc degrees in Materials Engineering from AGH University of Science and Technology in Kraków, Poland. He is currently a Ph.D. student in the Group of Wilson Smith at Delft University of Technology, Netherlands. He studies materials and devices for solar water splitting (www.smithsolarlab.com).

Dr. Henning Döscher is a senior scientist at Fraunhofer Institute for Systems and Innovation Research. He received his doctorate in Physics from Humboldt-Universität Berlin based on research at Helmholtz-Zentrum Berlin (2010). As a Marie-Curie-Fellow of the European Union, he joined the National Renewable Energy Laboratory (2012) and Philipps-Universität Marburg (2014) (www.isi.fraunhofer.de).

Dr. Wilson A. Smith is an Associate Professor of Chemical Engineering at Delft University of Technology. He earned his Ph.D. in Physics from the University of Georgia in 2010 before becoming a postdoctoral research associate at the Universite Pierre et Marie Curie/Sorbonne. In 2012 he began his independent career at TU Delft where his group studies materials and systems for renewable energy conversion and storage (www.smithsolarlab.com).

Dr. Morgan Stefik is an Assistant Professor of Chemistry and Biochemistry and the founding director of the South Carolina SAXS Collaborative at the University of South Carolina. His education spanned from Cal Poly SLO, to Cornell University, and EPFL. His group focuses on nanomaterials chemistry using block copolymers and ALD (www.stefikgroup.com).

■ ACKNOWLEDGMENTS

■ REFERENCES
(1) Kudo, A.; Ueda, K.; Kato, H.; Mikami, I. Photocatalytic O$_2$ Evolution under Visible Light Irradiation on BiVO$_4$ in Aqueous AgNO$_3$ Solution. *Catal. Lett.* **1998**, *53*, 229−230.

(2) Tokunaga, S.; Kato, H.; Kudo, A. Selective Preparation of Monoclinic and Tetragonal BiVO$_4$ with Scheelite Structure and Their Photocatalytic Properties. *Chem. Mater.* **2001**, *13*, 4624−4628.

(3) Park, Y.; McDonald, K. J.; Choi, K.-S. Progress in Bismuth Vanadate Photoanodes for Use in Solar Water Oxidation. *Chem. Soc. Rev.* **2013**, *42*, 2321−2337.

(4) Cooper, J. K.; Gul, S.; Toma, F. M.; Chen, L.; Liu, Y.-S.; Guo, J.; Ager, J. W.; Yano, J.; Sharp, I. D. Indirect Bandgap and Optical Properties of Monoclinic Bismuth Vanadate. *J. Phys. Chem. C* **2015**, *119*, 2969−2974.

(5) Walter, M. G.; Warren, E. L.; McKone, J. R.; Boettcher, S. W.; Mi, Q.; Santori, E. A.; Lewis, N. S. Solar Water Splitting Cells. *Chem. Rev.* **2010**, *110*, 6446−6473.

(6) Kim, T. W.; Ping, Y.; Galli, G. A.; Choi, K.-S. Simultaneous Enhancements in Photon Absorption and Charge Transport of Bismuth Vanadate Photoanodes for Solar Water Splitting. *Nat. Commun.* **2015**, *6*, 8769.

(7) Pihosh, Y.; Turkevych, I.; Mawatari, K.; Uemura, J.; Kazoe, Y.; Kosar, S.; Makita, K.; Sugaya, T.; Matsui, T.; Fujita, D.; et al. Photocatalytic Generation of Hydrogen by Core-Shell WO_3/$BiVO_4$ Nanorods with Ultimate Water Splitting Efficiency. *Sci. Rep.* **2015**, *5*, 11141.

(8) Kuang, Y.; Jia, Q.; Nishiyama, H.; Yamada, T.; Kudo, A.; Domen, K. A Front-Illuminated Nanostructured Transparent $BiVO_4$ Photoanode for > 2% Efficient Water Splitting. *Adv. Energy Mater.* **2016**, *6*, 1501645.

(9) Dotan, H.; Sivula, K.; Grätzel, M.; Rothschild, A.; Warren, S. C. Probing the Photoelectrochemical Properties of Hematite (α-Fe_2O_3) Electrodes Using Hydrogen Peroxide as a Hole Scavenger. *Energy Environ. Sci.* **2011**, *4*, 958−964.

(10) Zhong, D. K.; Choi, S.; Gamelin, D. R. Near-Complete Suppression of Surface Recombination in Solar Photoelectrolysis by "Co-Pi" Catalyst-Modified W:$BiVO_4$. *J. Am. Chem. Soc.* **2011**, *133*, 18370−18377.

(11) Liang, Y.; Tsubota, T.; Mooij, L. P. A.; van de Krol, R. Highly Improved Quantum Efficiencies for Thin Film $BiVO_4$ Photoanodes. *J. Phys. Chem. C* **2011**, *115*, 17594−17598.

(12) Abdi, F. F.; Van De Krol, R. Nature and Light Dependence of Bulk Recombination in Co-Pi-Catalyzed $BiVO_4$ Photoanodes. *J. Phys. Chem. C* **2012**, *116*, 9398−9404.

(13) Abdi, F. F.; Savenije, T. J.; May, M. M.; Dam, B.; van de Krol, R. The Origin of Slow Carrier Transport in $BiVO_4$ Thin Film Photoanodes: A Time-Resolved Microwave Conductivity Study. *J. Phys. Chem. Lett.* **2013**, *4*, 2752−2757.

(14) Ravensbergen, J.; Abdi, F. F.; van Santen, J. H.; Frese, R. N.; Dam, B.; van de Krol, R.; Kennis, J. T. M. Unraveling the Carrier Dynamics of $BiVO_4$: A Femtosecond to Microsecond Transient Absorption Study. *J. Phys. Chem. C* **2014**, *118*, 27793−27800.

(15) Butler, K. T.; Dringoli, B. J.; Zhou, L.; Rao, P. M.; Walsh, A.; Titova, L. V. Ultrafast Carrier Dynamics in $BiVO_4$ Thin Film Photoanode Material: Interplay between Free Carriers, Trapped Carriers and Low-Frequency Lattice Vibrations. *J. Mater. Chem. A* **2016**, *4*, 18516−18523.

(16) Suzuki, Y.; Murthy, D. H. K.; Matsuzaki, H.; Furube, A.; Wang, Q.; Hisatomi, T.; Domen, K.; Seki, K. Rational Interpretation of Correlated Kinetics of Mobile and Trapped Charge Carriers: Analysis of Ultrafast Carrier Dynamics in $BiVO_4$. *J. Phys. Chem. C* **2017**, *121*, 19044−19052.

(17) Ma, Y.; Pendlebury, S. R.; Reynal, A.; Le Formal, F.; Durrant, J. R. Dynamics of Photogenerated Holes in Undoped $BiVO_4$ Photoanodes for Solar Water Oxidation. *Chem. Sci.* **2014**, *5*, 2964−2973.

(18) Kim, T. W.; Choi, K.-S. Nanoporous $BiVO_4$ Photoanodes with Dual-Layer Oxygen Evolution Catalysts for Solar Water Splitting. *Science* **2014**, *343*, 990−994.

(19) Zachäus, C.; Abdi, F. F.; Peter, L. M.; van de Krol, R. Photocurrent of $BiVO_4$ Is Limited by Surface Recombination, Not Surface Catalysis. *Chem. Sci.* **2017**, *8*, 3712−3719.

(20) Abdi, F. F.; Han, L.; Smets, A. H. M.; Zeman, M.; Dam, B.; van de Krol, R. Efficient Solar Water Splitting by Enhanced Charge Separation in a Bismuth Vanadate-Silicon Tandem Photoelectrode. *Nat. Commun.* **2013**, *4*, 2195.

(21) Tolod, K.; Hernández, S.; Russo, N. Recent Advances in the $BiVO_4$ Photocatalyst for Sun-Driven Water Oxidation: Top-Performing Photoanodes and Scale-Up Challenges. *Catalysts* **2017**, *7*, 13.

(22) Tan, H. L.; Amal, R.; Ng, Y. H. Alternative Strategies in Improving the Photocatalytic and Photoelectrochemical Activities of Visible Light-Driven $BiVO_4$: A Review. *J. Mater. Chem. A* **2017**, *5*, 16498−16521.

(23) Luo, W.; Li, Z.; Yu, T.; Zou, Z. Effects of Surface Electrochemical Pretreatment on the Photoelectrochemical Performance of Mo-Doped $BiVO_4$. *J. Phys. Chem. C* **2012**, *116*, 5076−5081.

(24) Wang, G.; Ling, Y.; Lu, X.; Qian, F.; Tong, Y.; Zhang, J. Z.; Lordi, V.; Rocha Leao, C.; Li, Y. Computational and Photoelectrochemical Study of Hydrogenated Bismuth Vanadate. *J. Phys. Chem. C* **2013**, *117*, 10957−10964.

(25) Singh, A. P.; Kodan, N.; Dey, A.; Krishnamurthy, S.; Mehta, B. R. Improvement in the Structural, Optical, Electronic and Photo-electrochemical Properties of Hydrogen Treated Bismuth Vanadate Thin Films. *Int. J. Hydrogen Energy* **2015**, *40*, 4311−4319.

(26) Cooper, J. K.; Scott, S. B.; Ling, Y.; Yang, J.; Hao, S.; Li, Y.; Toma, F. M.; Stutzmann, M.; Lakshmi, K. V.; Sharp, I. D. Role of Hydrogen in Defining the N-Type Character of $BiVO_4$ Photoanodes. *Chem. Mater.* **2016**, *28*, 5761−5771.

(27) Jang, J.-W.; Friedrich, D.; Müller, S.; Lamers, M.; Hempel, H.; Lardhi, S.; Cao, Z.; Harb, M.; Cavallo, L.; Heller, R.; et al. Enhancing Charge Carrier Lifetime in Metal Oxide Photoelectrodes through Mild Hydrogen Treatment. *Adv. Energy Mater.* **2017**, *7*, 1701536.

(28) Li, T.; He, J.; Peña, B.; Berlinguette, C. P. Curing $BiVO_4$ Photoanodes with Ultraviolet Light Enhances Photoelectrocatalysis. *Angew. Chem., Int. Ed.* **2016**, *55*, 1769−1772.

(29) Trześniewski, B. J.; Smith, W. A. Photocharged $BiVO_4$ Photoanodes for Improved Solar Water Splitting. *J. Mater. Chem. A* **2016**, *4*, 2919−2926.

(30) Trześniewski, B. J.; Digdaya, I. A.; Nagaki, T.; Ravishankar, S.; Herraiz-Cardona, I.; Vermaas, D. A.; Longo, A.; Gimenez, S.; Smith, W. A. Near-Complete Suppression of Surface Losses and Total Internal Quantum Efficiency in $BiVO_4$ Photoanodes. *Energy Environ. Sci.* **2017**, *10*, 1517−1529.

(31) Liu, E. Y.; Thorne, J. E.; He, Y.; Wang, D. Understanding Photocharging Effects on Bismuth Vanadate. *ACS Appl. Mater. Interfaces* **2017**, *9*, 22083−22087.

(32) Lamm, B.; Sarkar, A.; Stefik, M. Surface Functionalized Atomic Layer Deposition of Bismuth Vanadate for Single-Phase Scheelite. *J. Mater. Chem. A* **2017**, *5*, 6060−6069.

(33) Ding, J.; Dai, Z.; Tian, F.; Zhou, B.; Zhao, B.; Zhao, H.; Chen, Z.; Liu, Y.; Chen, R. Generation of $V_{Br}^{\bullet}V_{Bi}'''V_O^{\bullet\bullet}$ Defect Cluster for $^1O_2$ Production in Molecular Oxygen Activation of Photocatalysis. *J. Mater. Chem. A* **2017**, *5*, 23453.

(34) Parmar, K. P. S.; Kang, H. J.; Bist, A.; Dua, P.; Jang, J. S.; Lee, J. S. Photocatalytic and Photoelectrochemical Water Oxidation over Metal-Doped Monoclinic $BiVO_4$ Photoanodes. *ChemSusChem* **2012**, *5*, 1926−1934.

(35) Eisenberg, D.; Ahn, H. S.; Bard, A. J. Enhanced Photo-electrochemical Water Oxidation on Bismuth Vanadate by Electro-deposition of Amorphous Titanium Dioxide. *J. Am. Chem. Soc.* **2014**, *136*, 14011−14014.

(36) Zhang, L.; Ye, X.; Boloor, M.; Poletayev, A.; Melosh, N. A.; Chueh, W. C. Significantly Enhanced Photocurrent for Water Oxidation in Monolithic Mo:$BiVO_4$/SnO_2/Si by Thermally Increasing the Minority Carrier Diffusion Length. *Energy Environ. Sci.* **2016**, *9*, 2044−2052.

(37) Gutkowski, R.; Khare, C.; Conzuelo, F.; Kayran, Y. U.; Ludwig, A.; Schuhmann, W. Unraveling Compositional Effects on the Light-Induced Oxygen Evolution in Bi(V−Mo−X)O_4 Material Libraries. *Energy Environ. Sci.* **2017**, *10*, 1213−1221.

(38) Kalanur, S. S.; Yoo, I.-H.; Park, J.; Seo, H. Insights into the Electronic Bands of WO_3/$BiVO_4$/TiO_2, Revealing High Solar Water Splitting Efficiency. *J. Mater. Chem. A* **2017**, *5*, 1455−1461.

(39) Shi, X.; Choi, I. Y.; Zhang, K.; Kwon, J.; Kim, D. Y.; Lee, J. K.; Oh, S. H.; Kim, J. K.; Park, J. H. Efficient Photoelectrochemical Hydrogen Production from Bismuth Vanadate-Decorated Tungsten Trioxide Helix Nanostructures. *Nat. Commun.* **2014**, *5*, 4775−4783.

(40) Galembeck, A.; Alves, O. L. $BiVO_4$ Thin Film Preparation by Metalorganic Decomposition. *Thin Solid Films* **2000**, *365*, 90−93.

(41) Seabold, J. A.; Choi, K.-S. Efficient and Stable Photo-Oxidation of Water by a Bismuth Vanadate Photoanode Coupled with an Iron Oxyhydroxide Oxygen Evolution Catalyst. *J. Am. Chem. Soc.* **2012**, *134*, 2186−2192.

(42) Chen, L.; Alarcón-Lladó, E.; Hettick, M.; Sharp, I. D.; Lin, Y.; Javey, A.; Ager, J. W. Reactive Sputtering of Bismuth Vanadate Photoanodes for Solar Water Splitting. *J. Phys. Chem. C* **2013**, *117*, 21635−21642.

(43) Gong, H.; Freudenberg, N.; Nie, M.; van de Krol, R.; Ellmer, K. $BiVO_4$ Photoanodes for Water Splitting with High Injection Efficiency, Deposited by Reactive Magnetron Co-Sputtering. *AIP Adv.* **2016**, *6*, 045108.

(44) Alarcón-Lladó, E.; Chen, L.; Hettick, M.; Mashouf, N.; Lin, Y.; Javey, A.; Ager, J. W. $BiVO_4$ Thin Film Photoanodes Grown by

Chemical Vapor Deposition. *Phys. Chem. Chem. Phys.* **2014**, *16*, 1651−1657.

(45) Stefik, M. Atomic Layer Deposition of Bismuth Vanadates for Solar Energy Materials. *ChemSusChem* **2016**, *9*, 1727−1735.

(46) Zhang, L.; Reisner, E.; Baumberg, J. J. Al-Doped ZnO Inverse Opal Networks as Efficient Electron Collectors in BiVO$_4$ Photoanodes for Solar Water Oxidation. *Energy Environ. Sci.* **2014**, *7*, 1402.

(47) Su, J.; Guo, L.; Bao, N.; Grimes, C. A. Nanostructured WO$_3$/BiVO$_4$ Heterojunction Films for Efficient Photoelectrochemical Water Splitting. *Nano Lett.* **2011**, *11*, 1928−1933.

(48) Zhou, L.; Zhao, C.; Giri, B.; Allen, P.; Xu, X.; Joshi, H.; Fan, Y.; Titova, L. V.; Rao, P. M. High Light Absorption and Charge Separation Efficiency at Low Applied Voltage from Sb-Doped SnO$_2$/BiVO$_4$ Core/Shell Nanorod-Array Photoanodes. *Nano Lett.* **2016**, *16*, 3463−3474.

(49) Zhou, L.; Yang, Y.; Zhang, J.; Rao, P. M. Photoanode with Enhanced Performance Achieved by Coating BiVO$_4$ onto ZnO-Templated Sb-Doped SnO$_2$ Nanotube Scaffold. *ACS Appl. Mater. Interfaces* **2017**, *9*, 11356−11362.

(50) *CRC Handbook of Chemistry and Physics*, 92nd ed.; Hayes, W., Lide, D. R., Eds.; Taylor & Francis: Boca Raton, FL, 2011.

(51) Schuisky, M.; Kukli, K.; Ritala, M.; Hårsta, A.; Leskelä, M. Atomic Layer CVD in the Bi−Ti−O System. *Chem. Vap. Deposition* **2000**, *6*, 139−145.

(52) Fidelsky, V.; Toroker, M. C. Enhanced Water Oxidation Catalysis of Nickel Oxyhydroxide through the Addition of Vacancies. *J. Phys. Chem. C* **2016**, *120*, 25405−25410.

(53) Diaz-Morales, O.; Ferrus-Suspedra, D.; Koper, M. T. M. The Importance of Nickel Oxyhydroxide Deprotonation on Its Activity towards Electrochemical Water Oxidation. *Chem. Sci.* **2016**, *7*, 2639−2645.

(54) Wang, G.; Ling, Y.; Wang, H.; Yang, X.; Wang, C.; Zhang, J. Z.; Li, Y. Hydrogen-Treated WO$_3$ Nanoflakes Show Enhanced Photostability. *Energy Environ. Sci.* **2012**, *5*, 6180.

(55) Wang, G.; Wang, H.; Ling, Y.; Tang, Y.; Yang, X.; Fitzmorris, R. C.; Wang, C.; Zhang, J. Z.; Li, Y. Hydrogen-Treated TiO$_2$ Nanowire Arrays for Photoelectrochemical Water Splitting. *Nano Lett.* **2011**, *11*, 3026−3033.

(56) Lu, X.; Wang, G.; Xie, S.; Shi, J.; Li, W.; Tong, Y.; Li, Y. Efficient Photocatalytic Hydrogen Evolution over Hydrogenated ZnO Nanorod Arrays. *Chem. Commun.* **2012**, *48*, 7717.

(57) Zhao, Z.; Li, Z.; Zou, Z. Structure and Energetics of Low-Index Stoichiometric Monoclinic Clinobisvanite BiVO$_4$ Surfaces. *RSC Adv.* **2011**, *1*, 874.

(58) Rossell, M. D.; Agrawal, P.; Borgschulte, A.; Hébert, C.; Passerone, D.; Erni, R. Direct Evidence of Surface Reduction in Monoclinic BiVO$_4$. *Chem. Mater.* **2015**, *27*, 3593−3600.

(59) Torruella, P.; Coll, C.; Martín, G.; López-Conesa, L.; Vila, M.; Díaz-Guerra, C.; Varela, M.; Ruiz-González, M. L.; Piqueras, J.; Peiró, F.; et al. Assessing Oxygen Vacancies in Bismuth Oxide through EELS Measurements and DFT Simulations. *J. Phys. Chem. C* **2017**, *121*, 24809.

(60) Pattengale, B.; Ludwig, J.; Huang, J. Atomic Insight into the W-Doping Effect on Carrier Dynamics and Photoelectrochemical Properties of BiVO$_4$ Photoanodes. *J. Phys. Chem. C* **2016**, *120*, 1421−1427.

(61) Nair, V.; Perkins, C. L.; Lin, Q.; Law, M. Textured Nanoporous Mo:BiVO$_4$ Photoanodes with High Charge Transport and Charge Transfer Quantum Efficiencies for Oxygen Evolution. *Energy Environ. Sci.* **2016**, *9*, 1412−1429.

(62) Qin, D.-D.; Wang, T.; Song, Y.-M.; Tao, C.-L. Reduced Monoclinic BiVO$_4$ for Improved Photoelectrochemical Oxidation of Water under Visible Light. *Dalt. Trans.* **2014**, *43*, 7691.

(63) Venkatesan, R.; Velumani, S.; Tabellout, M.; Errien, N.; Kassiba, A. Dielectric Behavior, Conduction and EPR Active Centres in BiVO$_4$ Nanoparticles. *J. Phys. Chem. Solids* **2013**, *74*, 1695−1702.

(64) Yin, W.-J.; Wei, S.-H.; Al-Jassim, M. M.; Turner, J.; Yan, Y. Doping Properties of Monoclinic BiVO$_4$ Studied by First-Principles Density-Functional Theory. *Phys. Rev. B: Condens. Matter Mater. Phys.* **2011**, *83*, 155102.

(65) Toma, F. M.; Cooper, J. K.; Kunzelmann, V.; McDowell, M. T.; Yu, J.; Larson, D. M.; Borys, N. J.; Abelyan, C.; Beeman, J. W.; Yu, K. M.; et al. Mechanistic Insights into Chemical and Photochemical Transformations of Bismuth Vanadate Photoanodes. *Nat. Commun.* **2016**, *7*, 12012.

(66) Rettie, A. J. E.; Chemelewski, W. D.; Emin, D.; Mullins, C. B. Unravelling Small-Polaron Transport in Metal Oxide Photoelectrodes. *J. Phys. Chem. Lett.* **2016**, *7*, 471−479.

(67) Kweon, K. E.; Hwang, G. S. Surface Structure and Hole Localization in Bismuth Vanadate: A First Principles Study. *Appl. Phys. Lett.* **2013**, *103*, 131603.

(68) Liang, Y.; Messinger, J. Improving BiVO$_4$ Photoanodes for Solar Water Splitting through Surface Passivation. *Phys. Chem. Chem. Phys.* **2014**, *16*, 12014.

(69) McDowell, M. T.; Lichterman, M. F.; Spurgeon, J. M.; Hu, S.; Sharp, I. D.; Brunschwig, B. S.; Lewis, N. S. Improved Stability of Polycrystalline Bismuth Vanadate Photoanodes by Use of Dual-Layer Thin TiO$_2$/Ni Coatings. *J. Phys. Chem. C* **2014**, *118*, 19618−19624.

(70) Jeon, T. H.; Choi, W.; Park, H. Cobalt−phosphate Complexes Catalyze the Photoelectrochemical Water Oxidation of BiVO$_4$ Electrodes. *Phys. Chem. Chem. Phys.* **2011**, *13*, 21392.

(71) Lai, Y.-H. H.; Palm, D. W.; Reisner, E. Multifunctional Coatings from Scalable Single Source Precursor Chemistry in Tandem Photoelectrochemical Water Splitting. *Adv. Energy Mater.* **2015**, *5*, 1501668.

(72) Choi, S. K.; Choi, W.; Park, H. Solar Water Oxidation Using Nickel-Borate Coupled BiVO$_4$ Photoelectrodes. *Phys. Chem. Chem. Phys.* **2013**, *15*, 6499.

(73) Ding, C.; Shi, J.; Wang, D.; Wang, Z.; Wang, N.; Liu, G.; Xiong, F.; Li, C. Visible Light Driven Overall Water Splitting Using cocatalyst/BiVO$_4$ Photoanode with Minimized Bias. *Phys. Chem. Chem. Phys.* **2013**, *15*, 4589.

(74) Li, M.; Luo, W.; Liu, B.; Zhao, X.; Li, Z.; Chen, D.; Yu, T.; Xie, Z.; Zhang, R.; Zou, Z. Remarkable Enhancement in Photocurrent of In$_{0.20}$Ga$_{0.80}$N Photoanode by Using an Electrochemical Surface Treatment. *Appl. Phys. Lett.* **2011**, *99*, 112108.

(75) Sayama, K.; Nomura, A.; Arai, T.; Sugita, T.; Abe, R.; Oi, T.; Iwasaki, Y.; Abe, Y.; Sugihara, H. Photoelectrochemical Decomposition of Water into H$_2$ and O$_2$ on Porous BiVO$_4$ Thin-Film Electrodes under Visible Light and Significant Effect of Ag Ion Treatment. *J. Phys. Chem. B* **2006**, *110*, 11352−11360.

(76) Walsh, A.; Yan, Y.; Huda, M. N.; Al-Jassim, M. M.; Wei, S.-H. Band Edge Electronic Structure of BiVO$_4$: Elucidating the Role of the Bi S and V D Orbitals. *Chem. Mater.* **2009**, *21*, 547−551.

(77) Rajeshwar, K. Fundamentals of Semiconductor Electrochemistry and Photoelectrochemistry. In *Encyclopedia of Electrochemistry*; Wiley-VCH Verlag GmbH & Co. KGaA: Weinheim, Germany, 2007; pp 1−51.

(78) Starr, D. E.; Favaro, M.; Abdi, F. F.; Bluhm, H.; Crumlin, E. J.; van de Krol, R. Combined Soft and Hard X-Ray Ambient Pressure Photoelectron Spectroscopy Studies of Semiconductor/electrolyte Interfaces. *J. Electron Spectrosc. Relat. Phenom.* **2017**, *221*, 106.

(79) Jovic, V.; Laverock, J.; Rettie, A. J. E.; Zhou, J.-S.; Mullins, C. B.; Singh, V. R.; Lamoureux, B.; Wilson, D.; Su, T.-Y.; Jovic, B.; et al. Soft X-Ray Spectroscopic Studies of the Electronic Structure of M:BiVO$_4$ (M = Mo, W) Single Crystals. *J. Mater. Chem. A* **2015**, *3*, 23743−23753.

(80) Favaro, M.; Abdi, F. F.; Lamers, M.; Crumlin, E. J.; Liu, Z.; van de Krol, R.; Starr, D. E. Light-Induced Surface Reactions at the Bismuth Vanadate/Potassium Phosphate Interface. *J. Phys. Chem. B* **2017**, DOI: 10.1021/acs.jpcb.7b06942.

(81) Döscher, H.; Geisz, J. F.; Deutsch, T. G.; Turner, J. A. Sunlight Absorption in Water − Efficiency and Design Implications for Photoelectrochemical Devices. *Energy Environ. Sci.* **2014**, *7*, 2951−2956.

(82) Shockley, W.; Queisser, H. J. Detailed Balance Limit of Efficiency of P-n Junction Solar Cells. *J. Appl. Phys.* **1961**, *32*, 510−519.

(83) Young, J. L.; Steiner, M. A.; Döscher, H.; France, R. M.; Turner, J. A.; Deutsch, T. G. Direct Solar-to-Hydrogen Conversion via Inverted Metamorphic Multi-Junction Semiconductor Architectures. *Nat. Energy* **2017**, *2*, 17028.

(84) Zhou, M.; Bao, J.; Bi, W.; Zeng, Y.; Zhu, R.; Tao, M.; Xie, Y. Efficient Water Splitting via a Heteroepitaxial BiVO$_4$ Photoelectrode Decorated with Co-Pi Catalysts. *ChemSusChem* **2012**, *5*, 1420−1425.

(85) Garner, L. E.; Steirer, K. X.; Young, J. L.; Anderson, N. C.; Miller, E. M.; Tinkham, J. S.; Deutsch, T. G.; Sellinger, A.; Turner, J. A.; Neale, N. R. Covalent Surface Modification of Gallium Arsenide Photo-cathodes for Water Splitting in Highly Acidic Electrolyte. *ChemSusChem* **2017**, *10*, 767−773.

(86) Döscher, H.; Young, J. L.; Geisz, J. F.; Turner, J. A.; Deutsch, T. G. Solar-to-Hydrogen Efficiency: Shining Light on Photoelectrochemical Device Performance. *Energy Environ. Sci.* **2016**, *9*, 74−80.

(87) Zhang, K.; Ma, M.; Li, P.; Wang, D. H.; Park, J. H. Water Splitting Progress in Tandem Devices: Moving Photolysis beyond Electrolysis. *Adv. Energy Mater.* **2016**, *6*, 1600602.

(88) Hardcastle, F. D.; Wachs, I. E.; Eckert, H.; Jefferson, D. A. Vanadium (V) Environments in Bismuth Vanadates: A Structural Investigation Using Raman Spectroscopy and Solid State ^{51}V NMR. *J. Solid State Chem.* **1991**, *90*, 194−210.

(89) Morgan, K.; Sayer, B. G.; Schrobilgen, G. J. Bismuth NMR Spectroscopy: ^{209}Bi and ^{19}F High-Resolution NMR Spectra of the hexafluorobismuthate(V) Ion. *J. Magn. Reson.* **1983**, *52*, 139−142.

(90) Hamaed, H.; Laschuk, M. W.; Terskikh, V. V.; Schurko, R. W. Application of Solid-State ^{209}Bi NMR to the Structural Characterization of Bismuth-Containing Materials. *J. Am. Chem. Soc.* **2009**, *131*, 8271−8279.

(91) Frost, R. L.; Henry, D. A.; Weier, M. L.; Martens, W. Raman Spectroscopy of Three Polymorphs of $BiVO_4$: Clinobisvanite, Dreyerite and Pucherite, with Comparisons to $(VO_4)_3$-Bearing Minerals: Namibite, Pottsite and Schumacherite. *J. Raman Spectrosc.* **2006**, *37*, 722−732.

(92) Tate, M. L.; Blom, D. A.; Avdeev, M.; Brand, H. E. A.; McIntyre, G. J.; Vogt, T.; Evans, I. R. New Apatite-Type Oxide Ion Conductor, $Bi_2La_8[(GeO_4)_6]O_3$: Structure, Properties, and Direct Imaging of Low-Level Interstitial Oxygen Atoms Using Aberration-Corrected Scanning Transmission Electron Micr. *Adv. Funct. Mater.* **2017**, *27*, 1605625.

(93) Cooper, J. K.; Gul, S.; Toma, F. M.; Chen, L.; Glans, P.-A.; Guo, J.; Ager, J. W.; Yano, J.; Sharp, I. D. Electronic Structure of Monoclinic $BiVO_4$. *Chem. Mater.* **2014**, *26*, 5365−5373.

(94) Resasco, J.; Zhang, H.; Kornienko, N.; Becknell, N.; Lee, H.; Guo, J.; Briseno, A. L.; Yang, P. TiO_2/$BiVO_4$ Nanowire Heterostructure Photoanodes Based on Type II Band Alignment. *ACS Cent. Sci.* **2016**, *2*, 80−88.